ARTICLE
PUBLISHED ONLINE: 31 AUGUST 2015 | DOI: 10.1038/NCHEMBIO.1906
nature chemical biology

Extracellular 4′-phosphopantetheine is a source for intracellular coenzyme A synthesis

Balaji Srinivasan[1], Madina Baratashvili[1], Marianne van der Zwaag[1], Bart Kanon[1], Cristina Colombelli[2], Roald A Lambrechts[1], Onno Schaap[1], Ellen A Nollen[3], Ajda Podgoršek[4], Gregor Kosec[4], Hrvoje Petković[4], Susan Hayflick[5], Valeria Tiranti[2], Dirk-Jan Reijngoud[6], Nicola A Grzeschik[1] & Ody C M Sibon[1]*

The metabolic cofactor coenzyme A (CoA) gained renewed attention because of its roles in neurodegeneration, protein acetylation, autophagy and signal transduction. The long-standing dogma is that eukaryotic cells obtain CoA exclusively via the uptake of extracellular precursors, especially vitamin B5, which is intracellularly converted through five conserved enzymatic reactions into CoA. This study demonstrates an alternative mechanism that allows cells and organisms to adjust intracellular CoA levels by using exogenous CoA. Here CoA was hydrolyzed extracellularly by ectonucleotide pyrophosphatases to 4′-phosphopantetheine, a biologically stable molecule able to translocate through membranes via passive diffusion. Inside the cell, 4′-phosphopantetheine was enzymatically converted back to CoA by the bifunctional enzyme CoA synthase. Phenotypes induced by intracellular CoA deprivation were reversed when exogenous CoA was provided. Our findings answer long-standing questions in fundamental cell biology and have major implications for the understanding of CoA-related diseases and therapies.

CoA was identified more than 60 years ago[1], and as a carrier of acyl groups it is essential for more than 100 metabolic reactions. It is estimated that CoA is an obligatory cofactor for 9% of known enzymatic reactions[2]. CoA and acetyl-CoA influence levels of protein acetylation in various model organisms[3–5]. Protein acetylation is an essential post-translational modification catalyzed by acetyltransferases that use acetyl-CoA as their source[6]. Acetyl-CoA levels also affect autophagy[7,8], and CoA promotes oocyte survival in *Xenopus laevis* by binding to and activating calcium/calmodulin-dependent protein kinase II (CaMKII)[9]. Together, intracellular concentrations of acetyl-CoA and CoA are critical to a broad range of cellular processes[10].

Current thinking about how cells and organisms obtain this indispensable molecule originates from experiments performed in the 1950s[2,11], which showed how a specific sequence of enzymatic activities results in the formation of CoA *in vitro* when vitamin B5 is used as a substrate. These enzymes are, in order, pantothenate kinase (PANK), phosphopantothenoylcysteine synthetase (PPCS), phosphopantothenoylcysteine decarboxylase (PPCDC), phosphopantetheine adenylyltransferase (PPAT) and dephospho-CoA kinase (DPCK) (**Fig. 1a**). Later, genes encoding these enzymes were identified in a wide range of organisms[2,12–14]. In some organisms, including *Drosophila melanogaster*, mice and humans, PPAT and DPCK enzyme activities are carried out by a single bifunctional protein, referred to as CoA synthase, or COASY[12,13,15]. *In vitro* experiments have shown that in addition to vitamin B5, pantetheine can also be phosphorylated by pantothenate kinase activity, and the formed product, 4′-phosphopantetheine, can serve as a precursor for CoA[16]. However, direct evidence that cells take up intact pantetheine and use it for CoA biosynthesis is still lacking.

In addition to renewed interest in the CoA molecule and its cellular roles, attention is being paid to the biosynthetic route because of its connection with specific forms of neurodegeneration. Two enzymes in the CoA *de novo* biosynthetic route, PANK (first step) and COASY (last two steps), are associated with a neurodegenerative disease known as neurodegeneration with brain iron accumulation (NBIA)[17,18]. Mutations in the gene encoding PANK2 (one of four human genes encoding PANK proteins) cause an NBIA disorder called pantothenate kinase–associated neurodegeneration (PKAN)[18]. Affected individuals experience progressive dystonia and accumulate iron in specific brain regions. Recently, individuals with mutations in the gene encoding COASY were identified and found to have similar clinical features and brain iron accumulation. This new NBIA disorder is referred to as COASY protein-associated neurodegeneration[17]. This strongly suggests that impairment of the classic CoA biosynthetic route underlies progressive neurodegeneration in these patient groups. Currently there is no treatment available to halt or reverse the neurodegeneration in people with these CoA-related disorders.

CoA levels are decreased in a *Drosophila* model of PKAN, and the neurodegenerative phenotypes and decreased CoA levels seen in this model are rescued by the addition of pantethine to the food[19]. Pantethine addition also rescues a ketogenic diet–induced neurodegenerative phenotype in *Pank2*$^{-/-}$ mice[20]. These studies demonstrate that in a pantothenate kinase–impaired background, CoA precursors other than vitamin B5 can alleviate neurodegenerative symptoms. How pantethine exerts its rescuing function (especially in the mouse model) is unclear because pantethine is highly unstable in serum and is rapidly converted into vitamin B5 and cysteamine by pantetheinases[20,21].

The aim of the current study was to determine whether there are alternative routes by which cells and organisms can obtain CoA. We found that extracellular CoA levels influenced intracellular CoA levels both *in vitro* and *in vivo*, although the CoA molecule was

[1]Department of Cell Biology, University Medical Center Groningen, University of Groningen, Groningen, the Netherlands. [2]Unit of Molecular Neurogenetics, Foundation IRCCS Neurological Institute C. Besta, Milan, Italy. [3]European Research Institute for the Biology of Aging, University of Groningen, Groningen, the Netherlands. [4]Acies Bio d.o.o., Ljubljana, Slovenia. [5]Departments of Molecular and Medical Genetics, Pediatrics, and Neurology, Oregon Health & Science University, Portland, Oregon, USA. [6]Department of Laboratory Medicine, Center for Liver Digestive and Metabolic Diseases, University Medical Center Groningen, Groningen, the Netherlands. *e-mail: o.c.m.sibon@umcg.nl

not biologically stable and cells did not take up CoA directly. We present evidence that ectonucleotide pyrophosphatases (ENPPs) hydrolyzed CoA into 4′-phosphopantetheine. In contrast to pantetheine[21], 4′-phosphopantetheine was stable in serum, was taken up by cells via passive diffusion and was intracellularly reconverted into CoA. Via this route, exogenous CoA rescued CoA-deprived phenotypes at the cellular, developmental, organismal and behavioral levels. We show that CoA rescue was independent of the first three classic CoA biosynthetic steps (involving PANK, PPCS and PPCDC, respectively) and depended on the last bifunctional enzyme, COASY. Our data demonstrate the existence of an alternative mechanism by which cells and organisms can influence intracellular CoA levels through the use of an extracellular CoA source with 4′-phosphopantetheine as the key intermediate.

RESULTS

CoA supplementation rescues CoA-depleted phenotypes

To learn whether cells are able to obtain CoA from sources other than classic *de novo* biosynthesis (**Fig. 1a**), we first sought to determine whether extracellular sources of CoA can serve as a supply for intracellular CoA. For this, we used RNA interference (RNAi) to induce PANK depletion to block the *de novo* biosynthesis route and create a CoA-depleted phenotype. Subsequently we tested the rescue potential of exogenous CoA. PANK depletion by RNAi in cultured *Drosophila* S2 cells (**Fig. 1b**) was associated with reductions in cell count (**Fig. 1b**,**c**) and histone acetylation (**Fig. 1d**,**e**), as previously demonstrated[4]. Addition of CoA to the medium of the cultured cells rescued the cell count in a concentration-dependent manner (**Fig. 1c**) and restored the histone acetylation phenotype (**Fig. 1f**). Next, we asked whether this rescue would also be observed in other cell types and systems with impaired CoA biosynthesis. Treating *Drosophila* S2 cells with the chemical PANK inhibitor hopantenate (HoPan)[22] also induced decreases in cell count (**Supplementary Results**, **Supplementary Fig. 1a**) and histone acetylation levels (**Supplementary Fig. 1b**,**c**). This HoPan-induced phenotype was also rescued by direct CoA supplementation to the cell medium (**Supplementary Fig. 1a**,**d**). Next we studied the effects of HoPan in mammalian HEK293 cells to address the possibility that the beneficial effects of exogenous CoA are specific to insect cells. When HEK293 cells were treated with HoPan, they showed a phenotype similar to that of treated *Drosophila* S2 cells, with decreased cell count and impaired histone acetylation. When CoA was added to the culture medium, both the decreased cell count (**Fig. 1g**) and the impaired histone acetylation (**Fig. 1h**) were rescued. These *in vitro* results confirmed the ability of exogenous CoA to rescue phenotypes induced by impaired PANK activity in diverse cellular systems.

To test the effect of CoA supplementation *in vivo*, we used homozygous *Caenorhabditis elegans* pantothenate kinase (*pnk-1*) mutants[4], which showed decreased motility (**Fig. 2a** and **Supplementary Fig. 2a**) and a decreased life span (**Fig. 2b**). Addition of CoA to the food of these mutants improved these phenotypes significantly (**Fig. 2a**,**b** and **Supplementary Fig. 2a**–**e**). Furthermore, when a *Drosophila* w^{1118} control fly line was treated with HoPan, larval lethality was induced, and a decreased rate of eclosion (emergence from the pupal case) was observed (**Fig. 2c**). This HoPan-induced phenotype was fully rescued by the addition of CoA to the food of the larvae (**Fig. 2d**).

These data demonstrate that supplementation with CoA rescued the phenotypes arising from impaired *de novo* CoA biosynthesis in diverse eukaryotic cell types and organisms.

External supply of CoA influences intracellular CoA

The rescue effect we observed could have occurred in several ways. Intracellular CoA levels could have been restored, or rescue could have been achieved independently of the restoration of CoA levels in the cells. In the latter case, intracellular levels of CoA would not have been restored by exogenous CoA. To investigate this, we developed a sensitive HPLC method consisting of precolumn thiol-specific derivatization of samples with ammonium 7-fluorobenzofurazan-4-sulfonate followed by chromatographic separation by gradient elution on a C18 column and fluorescence detection (Online Methods). The HPLC CoA analysis showed that intracellular CoA levels were significantly reduced in extracts of HoPan-treated S2 and HEK293 cells, and the addition of CoA to the culture medium restored the intracellular concentration of CoA (**Fig. 2e**,**f**). These results suggested that extracellular CoA exerted its beneficial effects in CoA-depleted cells by increasing and thereby 'normalizing' intracellular CoA concentrations.

In serum, CoA is degraded to stable 4′-phosphopantetheine

The mechanism behind this alternative CoA route was not known. The observations shown in **Figures 1** and **2** indicated that either (1) CoA entered cells directly, although such a transport process has not been described, or (2) CoA was converted to an intermediate product that entered the cell and was converted back to CoA in a PANK-independent manner. Previous research showed that CoA is not stable in liver extracts and degrades to 50% at −20 °C after a week[23]; however, the stability of CoA in an extracellular environment such as an aqueous or standard cell culture medium is unknown. Moreover, these early reports did not identify specific degraded or converted products. We measured the stability of CoA in PBS, serum-free medium, medium containing fetal calf serum (FCS), and FCS during a 3-h incubation. HPLC analysis showed that CoA was relatively stable in PBS and serum-free medium, with >95% of the initial concentration still present after 3 h (**Supplementary Figs. 3** and **4a**). However, in the presence of FCS, CoA was rapidly degraded (**Fig. 3a** and **Supplementary Fig. 4b**), and after 3 h of incubation, only 10% of the initial concentration was detectable (**Supplementary Figs. 3** and **4b**). Detailed stability analysis of CoA in PBS and FCS at different time points showed that 90% of CoA was degraded after only 30 min in FCS (**Fig. 3a**). The disappearance of CoA coincided with the appearance of one unknown thiol-containing product in the HPLC chromatogram, which migrated at 18.273 min and remained stable over the full 3-h time course (**Fig. 3b** and **Supplementary Fig. 4b**). Because this extra peak had to be a thiol-containing molecule, we speculated that it might be a product of CoA degradation, specifically, dephospho-CoA, 4′-phosphopantetheine or pantetheine[2]. In contrast to dephospho-CoA and pantetheine, 4′-phosphopantetheine is not commercially available, so we chemically synthesized this compound (**Supplementary Note**) in order to complete our analysis. HPLC analysis and comparison with standards demonstrated that the thiol-containing degradation product of CoA was neither dephospho-CoA nor pantetheine (**Supplementary Fig. 4**), but its retention time exactly matched that of the 4′-phosphopantetheine standard (**Fig. 3c**,**d** and **Supplementary Fig. 4b**,**c**). These results indicated that CoA was converted into 4′-phosphopantetheine in serum and was stable. This is in contrast to pantetheine, which is not stable in serum (**Supplementary Fig. 5a**)[21]. We further investigated the conversion of CoA in mouse serum and in human serum. In sera from both species, including serum derived from people with PKAN (**Supplementary Fig. 5b**), we found that CoA was converted to 4′-phosphopantetheine (**Fig. 3e** and **Supplementary Fig. 5c**).

To investigate whether this conversion also occurred *in vivo*, we fed CoA to *Drosophila* larvae and obtained L1- and L2-stage larval extracts after 2 and 3 d of feeding, respectively. HPLC analysis showed that the addition of CoA resulted in increased levels of 4′-phosphopantetheine in both L1 (>20-fold) and L2 (>60-fold) larvae (**Fig. 3f**). To investigate whether this conversion also occurred in higher organisms, we injected different concentrations of CoA intravenously into adult mice and collected plasma from the mice 30 min and 6 h after injection. HPLC analysis in

combination with mass spectrometry revealed the presence of low levels of endogenous 4′-phosphopantetheine in fresh mouse serum (**Supplementary Fig. 6a–c**) and showed that the injected CoA was rapidly converted to 4′-phosphopantetheine after 30 min (**Fig. 3g**). Moreover, mass spectrometry showed that elevated levels of 4′-phosphopantetheine were still present in the plasma 6 h after CoA injection (**Supplementary Fig. 6d**).

These data indicated that CoA is converted into 4′-phosphopantetheine *in vitro* and *in vivo*. Furthermore, these results suggested that 4′-phosphopantetheine could be the principal molecule taken up by CoA-depleted cells and converted into CoA intracellularly, and that this could result in the rescue of CoA-depleted phenotypes.

Conversion of CoA mediated by ENPPs

Next we asked which factors might be responsible for the conversion of CoA into 4′-phosphopantetheine in serum. To identify candidate enzymes, we preconditioned serum from various species (fetal calf, mouse and human) and assessed CoA conversion into 4′-phosphopantetheine. First we studied the effect of heat inactivation of the serum. HPLC analysis showed that heating the serum at 56 °C for 30 min completely abolished the conversion of CoA to 4′-phosphopantetheine (**Fig. 4a**), which indicated the involvement of enzymes or proteins in the process. The conversion of CoA to 4′-phosphopantetheine requires the hydrolysis of a phosphoanhydride bond, which is typically catalyzed by (pyro) phosphatases or hydrolases. The majority of enzymes in the known family of (pyro)phosphatases and hydrolases depend on metal ions for their activity. To test these candidates, we added EDTA to serum to chelate metal ions. Treatment of serum with EDTA completely prevented the formation of 4′-phosphopantetheine (**Fig. 4b**). This strongly suggested that metal ions were required for the CoA conversion. The most likely hydrolase or (pyro)phosphatase candidates that possess the ability to convert CoA and are metal-ion dependent for their activity are nudix hydrolases, alkaline phosphatases and ENPPs[24–28]. These candidate enzymes are also known for their ability to hydrolyze adenosine 5′-triphosphate (ATP) and adenosine 5′-diphosphate (ADP)[29–31]. Therefore, we tested the conversion of CoA into 4′-phosphopantetheine in serum after the addition of excess ATP and ADP. Both competitively blocked the conversion in all sera tested, further underscoring the involvement of one of these enzymes (**Fig. 4c**). Alkaline phosphatase and ENPPs are excreted by cells and are present in serum[29,32]. Nudix hydrolases are intracellular hydrolases of CoA[25,30]; however, an additional possible extracellular role for this class of hydrolases cannot be excluded.

Next, we used sodium fluoride (NaF) and levamisole to inhibit nudix hydrolases and

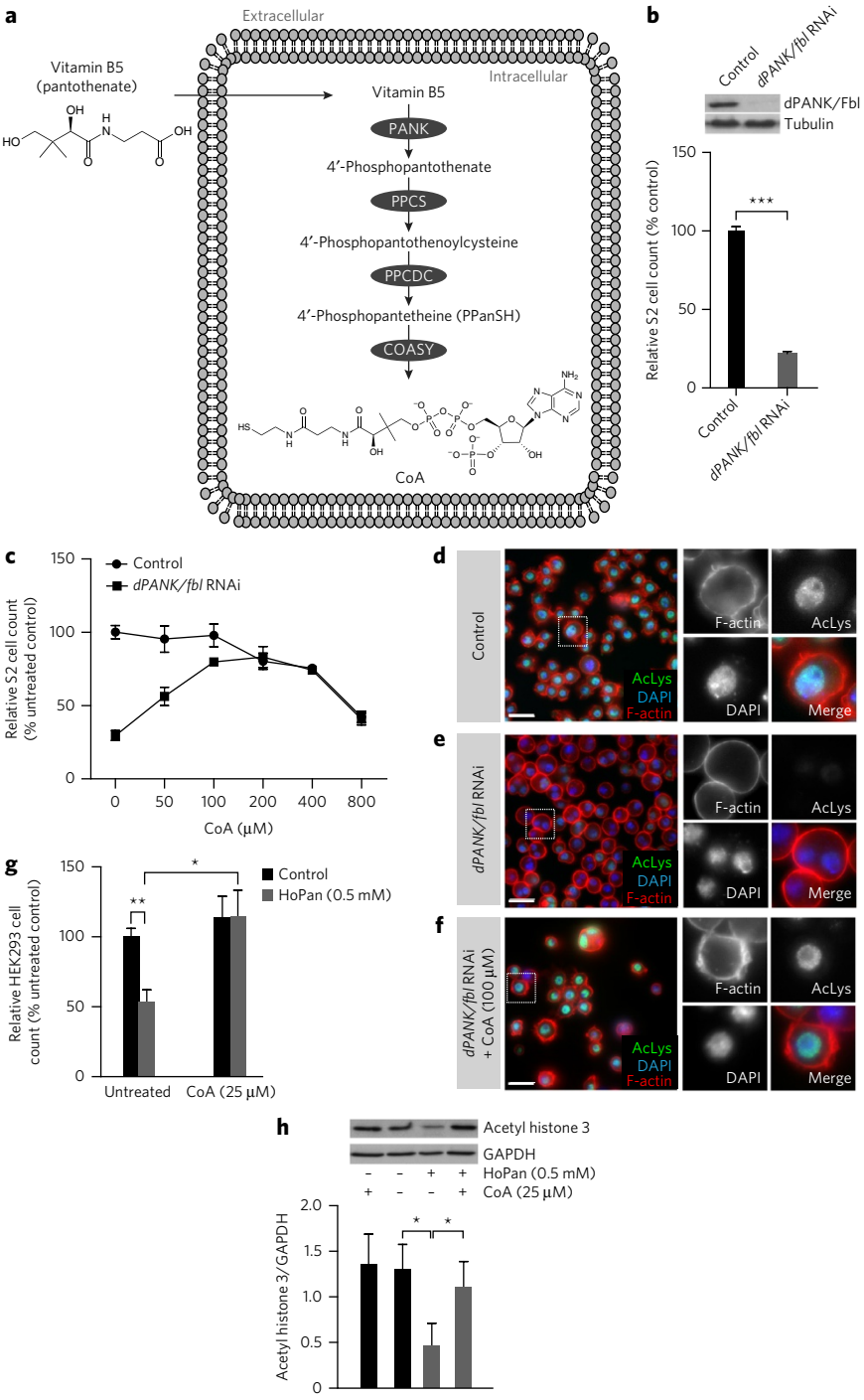

Figure 1 | CoA supplementation rescues PANK-impaired phenotypes. (**a**) Canonical *de novo* CoA biosynthesis pathway. Vitamin B5 (pantothenate) is taken up and intracellularly converted to CoA by the enzymes PANK, PPCS, PPCDC and COASY. (**b**) Relative *Drosophila* S2 cell counts for control (100%) and *dPANK/fbl* RNAi-treated cells. Inset shows a western blot of dPANK/Fbl protein levels in control and *dPANK/fbl* RNAi-treated cells, with tubulin as a loading control. Data are mean and s.d. ($n = 3$). (**c**) Relative counts of control and *dPANK/fbl* RNAi-treated cells in the presence of increasing concentrations of CoA. Data are mean ± s.d. ($n = 4$). (**d–f**) Immunofluorescence showing protein acetylation levels in control (**d**) and *dPANK/fbl* RNAi-treated cells without (**e**) and with (**f**) CoA. Anti-acetylated lysine (green; acLys), rhodamin-phalloidin (red; F-actin) and DAPI (blue; DNA) were used. Scale bars, 20 μm. (**g**) Relative counts of control (100%) and HoPan-treated HEK293 cells with and without CoA. Data are mean and s.d. ($n = 3$). (**h**) Western blot and quantification of histone acetylation levels in control and HoPan-treated HEK293 cells in the presence and absence of CoA. GAPDH was used as a loading control. Data are mean and s.d. ($n = 3$). $^*P \leq 0.05$, $^{**}P \leq 0.01$, $^{***}P \leq 0.001$, two-tailed unpaired Student's *t*-test.

alkaline phosphatase, respectively, and we also used two different ENPP inhibitors, suramin and 4,4′-diisothiocyanatostilbene-2,2′ disulfonic acid (DIDS)[33–35]. Our data showed that suramin and DIDS were able to efficiently abolish the degradation of CoA into 4′-phosphopantetheine in all the sera, unlike levamisole and NaF, which showed only mild and no inhibition of CoA degradation into 4′-phosphopantetheine, respectively (**Fig. 4d**). NaF did not influence CoA degradation in serum, which indicated that nudix hydrolases either were not present or did not degrade CoA in serum. These experiments implicated ENPPs as the most likely class of enzymes to hydrolyze CoA into 4′-phosphopantetheine in serum. Moreover, in all of the CoA serum stability experiments mentioned above, there was an inverse correlation between levels of CoA and 4′-phosphopantetheine (**Supplementary Fig. 7**), which supported the idea that CoA degradation into 4′-phosphopantetheine was mediated by ENPPs.

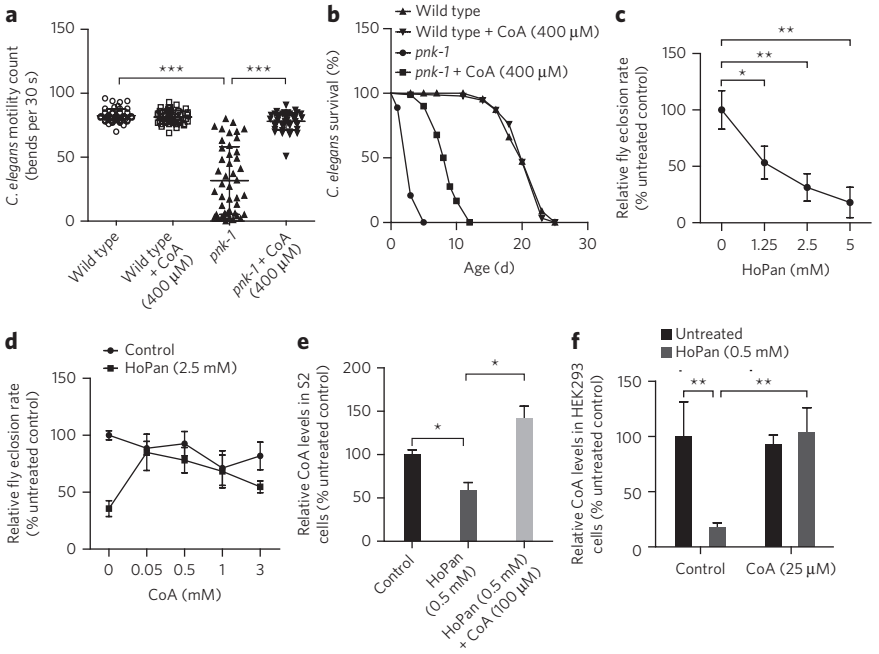

Figure 2 | CoA rescues impaired PANK phenotypes of *C. elegans* and *Drosophila*. (**a**) Motility was determined in *pnk-1* mutant and wild-type *C. elegans* with and without CoA treatment. Data are mean ± s.d.; each symbol represents an individual data point ($n = 45$). (**b**) Life-span analysis of *C. elegans pnk-1* mutants with ($n = 90$) and without ($n = 96$) CoA treatment compared with wild types with ($n = 92$) and without ($n = 83$) CoA treatment. Differences in survival curves were significant ($P < 0.001$, log-rank (Mantel-Cox) test) between untreated and CoA-treated *pnk-1* mutants. (**c**) Eclosion rates of adult control flies (set as 100%) and flies treated with increasing concentrations of HoPan added to the food during development. Data are mean ± s.d. ($n = 3$). (**d**) Relative eclosion rates of adult control flies and flies treated with 2.5 mM HoPan added to the food during development in the presence of increasing concentrations of CoA. Data are mean ± s.d. ($n = 3$). (**e**) Intracellular CoA levels measured by HPLC in *Drosophila* S2 control cells (100%) and cells treated with HoPan only or with HoPan and CoA. (**f**) Intracellular CoA levels measured by HPLC in HEK293 control cells (100%) and HoPan-treated cells with and without CoA. Data in **e** and **f** are mean and s.d. ($n = 3$). $^*P \leq 0.05$, $^{**}P \leq 0.01$, $^{***}P \leq 0.001$, two-tailed unpaired Student's *t*-test.

Rescue of CoA-depleted phenotypes

Our data so far showed that PANK impairment induced a decrease in CoA levels, and they also predicted a decrease in 4′-phosphopantetheine levels. Furthermore, they suggested that the addition of 4′-phosphopantetheine to CoA-depleted cells would rescue the induced phenotypes. HPLC analysis of HoPan-treated *Drosophila* S2 cells indeed showed reduced levels of 4′-phosphopantetheine, and external supplementation with either CoA or 4′-phosphopantetheine significantly increased intracellular levels of 4′-phosphopantetheine (**Fig. 5a**). Moreover, when 4′-phosphopantetheine was added to *Drosophila* S2 cells treated with HoPan (**Fig. 5b**) or *dPANK/fbl* RNAi (**Fig. 5c**), the CoA-depleted phenotype was again rescued. 4′-Phosphopantetheine supplementation also rescued the histone acetylation defect in *Drosophila* S2 cells treated with *dPANK/fbl* RNAi (**Supplementary Fig. 8a–c**) or HoPan (**Supplementary Fig. 8d–f**). Finally, we tested the rescue effect of 4′-phosphopantetheine in HoPan-treated mammalian HEK293 cells and found that it also rescued the HoPan-induced reductions in cell count (**Supplementary Fig. 8g**), intracellular CoA levels (**Supplementary Fig. 8h**) and histone acetylation levels (**Supplementary Fig. 8i**). Next we investigated whether intact 4′-phosphopantetheine entered cells and whether it was subsequently converted into CoA. First we treated intact cultured *Drosophila* S2 cells with stable isotope–labeled 4′-phosphopantetheine under various conditions and used mass spectrometry analysis to measure the levels of stable isotope–labeled CoA and 4′-phosphopantetheine (**Supplementary Fig. 9a–d**) in extracts from the harvested cells. When labeled 4′-phosphopantetheine was added to the cell culture medium, labeled CoA was detected in harvested cell extracts (**Fig. 5d**). In the presence of HoPan, CoA levels were decreased and replenished in the form of labeled CoA when labeled 4′-phosphopantetheine was added. These data demonstrated that exogenously provided 4′-phosphopantetheine was able to enter cells and was intracellularly converted into CoA under both normal culturing conditions and conditions of impaired CoA biosynthesis after treatment with HoPan. Next we investigated the characteristics of the passage of 4′-phosphopantetheine over the cell membrane. First, we incubated S2 cells cultured at 25 °C (the normal culturing temperature for these cells) and 4 °C with labeled 4′-phosphopantetheine. The cultured cells showed intracellular presence of the label within 30 min after incubation. There was no significant difference in intracellular levels of labeled 4′-phosphopantetheine between these two conditions (**Fig. 5e**). Next we investigated whether the levels of intracellular 4′-phosphopantetheine increased to the same extent as externally added increasing concentrations of 4′-phosphopantetheine under these conditions. We added increasing concentrations (10, 100 and 1,000 µM) of labeled 4′-phosphopantetheine to the cells (**Fig. 5f**). The results indicated that the capacity of the cells to accumulate externally provided 4′-phosphopantetheine was not influenced by temperature and was determined by the extracellular concentration. Finally, we investigated the membrane-permeating efficiency of 4′-phosphopantetheine using a parallel artificial membrane-permeability assay (PAMPA)[36]. In this assay, 4′-phosphopantetheine, but not CoA, showed membrane-permeating properties (**Supplementary Fig. 9e–f**). Together, these results pointed to a capacity of 4′-phosphopantetheine to permeate membranes via passive diffusion.

CoA rescues *dPANK/fbl* and *dPPCDC* phenotypes

Our data showed that CoA from external sources could be used to replenish intracellular CoA levels through its hydrolysis product

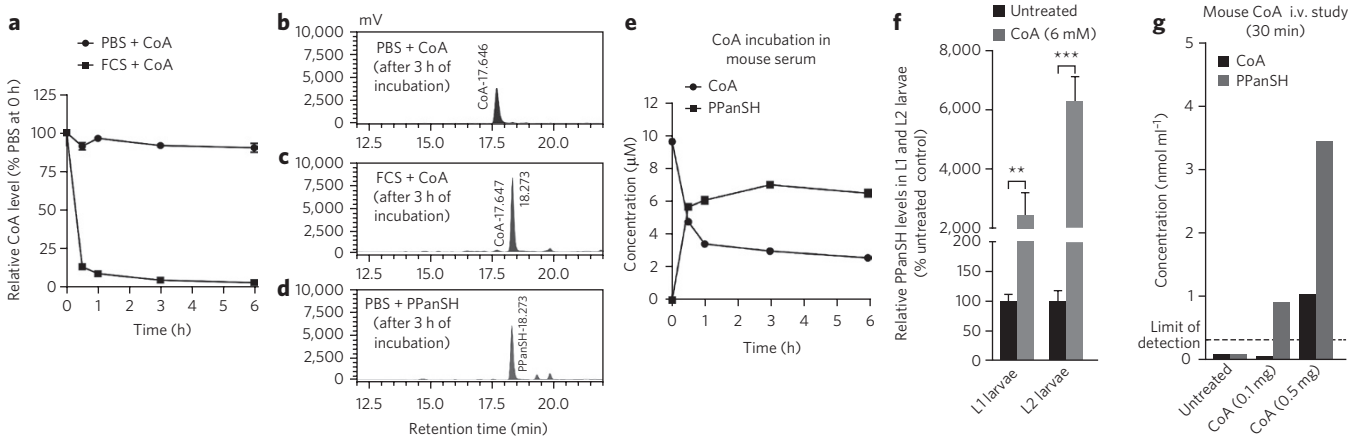

Figure 3 | CoA is converted into stable 4′-phosphopantetheine (PPanSH) *in vitro*, in serum and *in vivo* in *Drosophila* and mice. (**a**) Stability profile of CoA (determined by HPLC analysis) in PBS (100% at 0 h in PBS) and in FCS over the course of 6 h. Data represent mean ± s.d. ($n = 3$). (**b**,**c**) HPLC chromatogram profile of CoA incubated for 3 h in (**b**) PBS and in (**c**) FCS. (**d**) The retention time of standard PPanSH is identical to that of the observed conversion product of CoA in FCS. (**e**) Concentrations of CoA and PPanSH in mouse serum over 6 h after the addition of CoA, as determined by HPLC analysis. Data represent means ($n = 3$). (**f**) Relative PPanSH levels in *Drosophila* L1- and L2-stage larvae (determined by HPLC analysis) under untreated conditions (100%) and after feeding with CoA. Data are mean and s.d. ($n = 3$). $^{**}P \leq 0.01$, $^{***}P \leq 0.001$, two-tailed unpaired Student's *t*-test. (**g**) Concentrations of CoA and PPanSH in mouse serum (determined by HPLC analysis) 30 min after *in vivo* intravenous (i.v.) injection of various amounts of CoA. Data represent means ($n = 2$).

4′-phosphopantetheine and subsequent conversion back to CoA. The enzyme most likely to be involved in this conversion is the last bifunctional enzyme of the classic CoA biosynthetic pathway, COASY. This hypothesis (**Supplementary Fig. 10**) predicts that CoA, but not vitamin B5, can rescue phenotypes caused by mutations in genes encoding enzymes upstream of 4′-phosphopantetheine in the CoA pathway. As a corollary, CoA would not be predicted to rescue *COASY* mutant phenotypes.

We aimed to test this hypothesis. In the *Drosophila* genome, we identified single orthologues for all the enzymes involved in CoA biosynthesis[12], including *dPANK/fbl*, *dPPCDC* and *dCOASY*. We obtained a set of *Drosophila* strains carrying either mutations in genes encoding these enzymes or an upstream activation sequence (UAS)-RNAi construct. Homozygous mutants or flies ubiquitously expressing the RNAi construct showed downregulation of mRNA levels (**Supplementary Fig. 11**) or protein levels (**Supplementary Fig. 12a**) of these enzymes. CoA and 4′-phosphopantetheine levels were also significantly reduced in all conditions (**Supplementary Fig. 12b–e**), with the exception of *dCOASY* mutants, which showed a significant reduction of CoA but not of 4′-phosphopantetheine (**Supplementary Fig. 12f**).

It should be stressed that not all mutants with defects in CoA biosynthesis enzymes showed an identical phenotype, which can be explained by the types of fly lines (e.g., RNAi construct–expressing lines, hypomorphic or null mutants) used. This has been reported previously not only for *Drosophila* but also for other organisms[12,37]. Regardless of the severity of the phenotypes and the developmental stage in which they first arose, the determination of the rescue potential of CoA in the available mutants was a valuable tool for testing our hypothesis. A scheme of the hypothesis, the *Drosophila* life span and the phenotypes of the fly lines used are presented in **Supplementary Figure 10**.

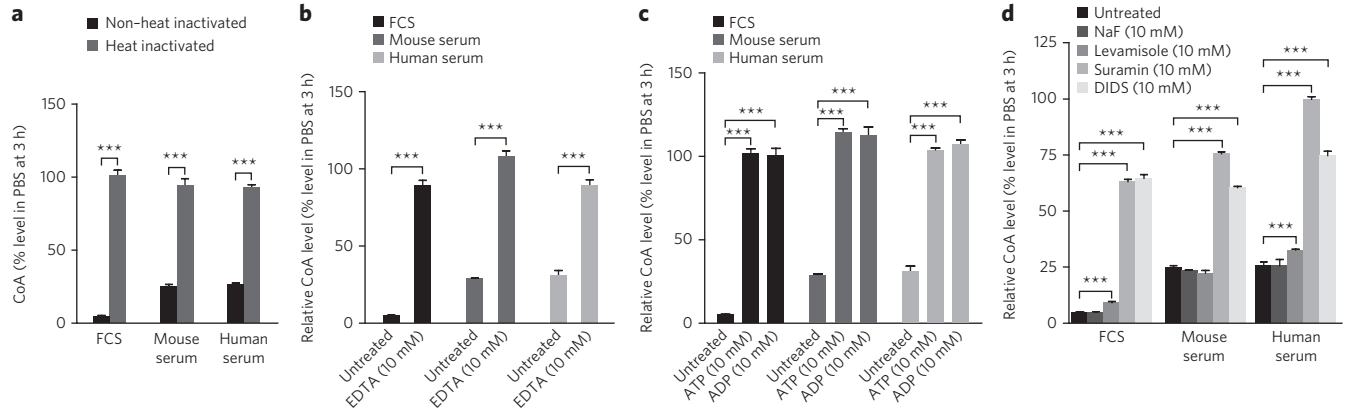

Figure 4 | Conversion of CoA into stable 4′-phosphopantetheine in serum is mediated by heat-unstable and metal-activated enzymes. (**a**) CoA stability as measured via HPLC analysis after 3 h of incubation in FCS, mouse serum and human serum. (**b**) CoA stability as determined by HPLC after 3 h of incubation in FCS, mouse serum and human serum pretreated with EDTA (10 mM) or not treated. (**c**) CoA levels after 3 h of incubation in FCS, mouse serum and human serum not treated or pretreated with ATP or ADP (both 10 mM). (**d**) CoA stability after 3 h of incubation in FCS, mouse serum and human serum not treated or pretreated with NaF, levamisole, suramin or DIDS (all 10 mM). Data are mean and s.d. ($n = 3$). $^{*}P \leq 0.05$, $^{**}P \leq 0.01$, $^{***}P \leq 0.001$, two-tailed unpaired Student's *t*-test. In all these experiments, CoA was added to the indicated sera to a final concentration of 10 μM (a detailed protocol is presented in the Online Methods).

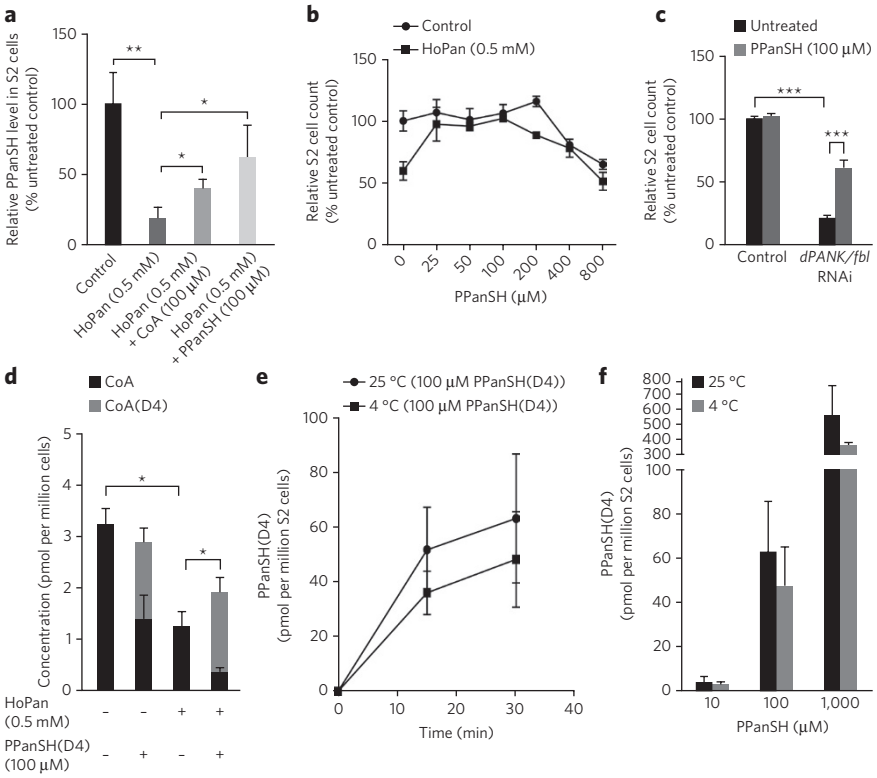

Figure 5 | External supplementation with 4′-phosphopantetheine (PPanSH) rescues CoA-deprived phenotypes. (**a**) Intracellular PPanSH levels (measured by HPLC analysis) in control *Drosophila* S2 cells (100%) and cells treated with HoPan (0.5 mM) with and without the addition of CoA or PPanSH (100 µM). (**b**) *Drosophila* S2 cell count in control cells and HoPan-treated cells under conditions of increasing PPanSH concentration. (**c**) Cell counts in control (100%) and *dPANK/fbl* RNAi-treated *Drosophila* S2 cells with and without PPanSH (100 µM) added to the medium. (**d**) Levels of unlabeled CoA and labeled CoA(D4) in S2 cells with and without HoPan (0.5 mM) incubated with stable isotope-labeled PPanSH(D4) (100 µM), as measured via mass spectrometry. Cumulative CoA and CoA(D4) levels were used for statistical analysis. (**e**) Levels of labeled compound in cell extracts from S2 cells incubated at 4 °C and 25 °C with stable isotope-labeled PPanSH(D4), as measured by mass spectrometry. (**f**) Levels of stable isotope-labeled PPanSH(D4) in S2 cell extracts after the addition of various concentrations to the cells, as measured by mass spectrometry. Data represent mean ± s.d. ($n = 3$). $^{*}P \leq 0.05$, $^{**}P \leq 0.01$, $^{***}P \leq 0.001$, two-tailed unpaired Student's *t*-test.

We first tested two available mutants for *dPANK/fbl*: the hypomorphic[19] *dPANK/fbl*^{1} and the null mutant *dPANK/fbl*^{null}. Homozygous *dPANK/fbl*^{1} mutants showed reduced levels of dPANK/Fbl protein, and in homozygous *dPANK/fbl*^{null} mutants levels of dPANK/Fbl protein were below detection (**Supplementary Fig. 12a**). Correlating with this, homozygous *dPANK/fbl*^{1} mutants showed a reduced adult life span (**Fig. 6a** and **Supplementary Fig. 13a**)[12,19], whereas homozygous *dPANK/fbl*^{null} mutants developed only until an early L2 larval stage, and pupae were not observed (**Fig. 6b**). Addition of CoA to the food of the homozygous *dPANK/fbl*^{1} mutants increased the life span from 20 d to 40 d (**Fig. 6a** and **Supplementary Fig. 13a**), and the addition of CoA to the food of homozygous *dPANK/fbl*^{null} mutants extended development from the L2 stage to early pupal development (**Fig. 6b**). These results supported our hypothesis. Remarkably, in *dPANK/fbl*^{null} mutants, we detected low levels of CoA and 4′-phosphopantetheine (**Supplementary Fig. 12c**). It is possible that these substances were obtained from a maternal supply or from the fly food (**Supplementary Fig. 13b**).

To compromise dPPCDC, the enzyme carrying out the third step of the CoA biosynthesis pathway, we used a UAS-RNAi line (*dPPCDC* RNAi) as well as a *dPPCDC* mutant and investigated rescue by CoA. Homozygous *dPPCDC* mutants showed lethality at early second-instar larval stage L2 (**Fig. 6c**). *dPPCDC* RNAi–expressing flies showed a milder phenotype in which adult flies were viable but had a reduced life span (**Fig. 6d**). Females also showed sterility associated with small ovaries, and no eggs were produced (**Fig. 6e** and **Supplementary Fig. 14a–d**). The addition of CoA to the food of homozygous *dPPCDC* mutants extended larval development to the late pupal stage (**Fig. 6c**). For the *dPPCDC* RNAi–expressing flies, supplementation of CoA to the food increased the maximal life span from 10 d to 30 d (**Fig. 6d** and **Supplementary Fig. 14e**). In addition, female sterility was rescued, as evidenced by observations of egg production and eclosion of viable offspring (**Fig. 6e**,**f** and **Supplementary Fig. 14c**,**d**). These results were also consistent with our hypothesis.

Finally, we tested a line with a mutant form of the bifunctional enzyme dCOASY downstream of 4′-phosphopantetheine. Homozygous *dCOASY* mutants developed until the first-instar larval stage, and the addition of CoA to the food did not result in significant rescue (**Fig. 6g**). As a negative control for all rescue experiments, we added vitamin B5 to the food; this did not result in any significant rescue of the phenotypes. A summary of the rescue effects observed with CoA in all fly lines is presented in **Supplementary Figure 10**.

To test our hypothesis further, we down-regulated *COASY* with RNAi in mammalian HEK293 cells. Under these conditions, levels of COASY, CoA and histone acetylation were significantly reduced ($P \leq 0.01$; **Supplementary Fig. 14f**,**g**). As in *dCOASY* mutants, levels of 4′-phosphopantetheine remained unaltered in COASY-compromised mammalian cells (**Supplementary Fig. 14g**). The addition of CoA to the medium neither rescued the *COASY* RNAi–induced decrease in intracellular CoA levels (**Supplementary Fig. 14g**) nor restored histone acetylation levels (**Supplementary Fig. 14f**). These results were also in agreement with our hypothesis.

Taken together, these results demonstrated that impairment of the CoA biosynthetic pathway by genetic manipulation can give rise to highly complex pleiotropic effects affecting life span, development and fecundity. These phenotypes can be (partially) rescued by the addition of CoA to the food of affected animals. The added CoA is hydrolyzed to 4′-phosphopantetheine, which crosses the plasma membrane via passive diffusion before being converted back to CoA intracellularly in a step requiring COASY (**Fig. 6h**).

DISCUSSION

In our study we addressed the basic question of whether cells and organisms have alternative ways to obtain the essential molecule CoA aside from the canonical pathway using vitamin B5. We found that cells and organisms were able to acquire exogenous CoA and convert it into the stable molecule 4′-phosphopantetheine, which entered cells and was converted again into CoA. This newly identified pathway for 4′-phosphopantetheine suggests that this molecule can serve as a transport form of CoA or a stable reservoir for rapid access and conversion. The proposed mechanism hypothetically allows a net flow of CoA or 4′-phosphopantetheine

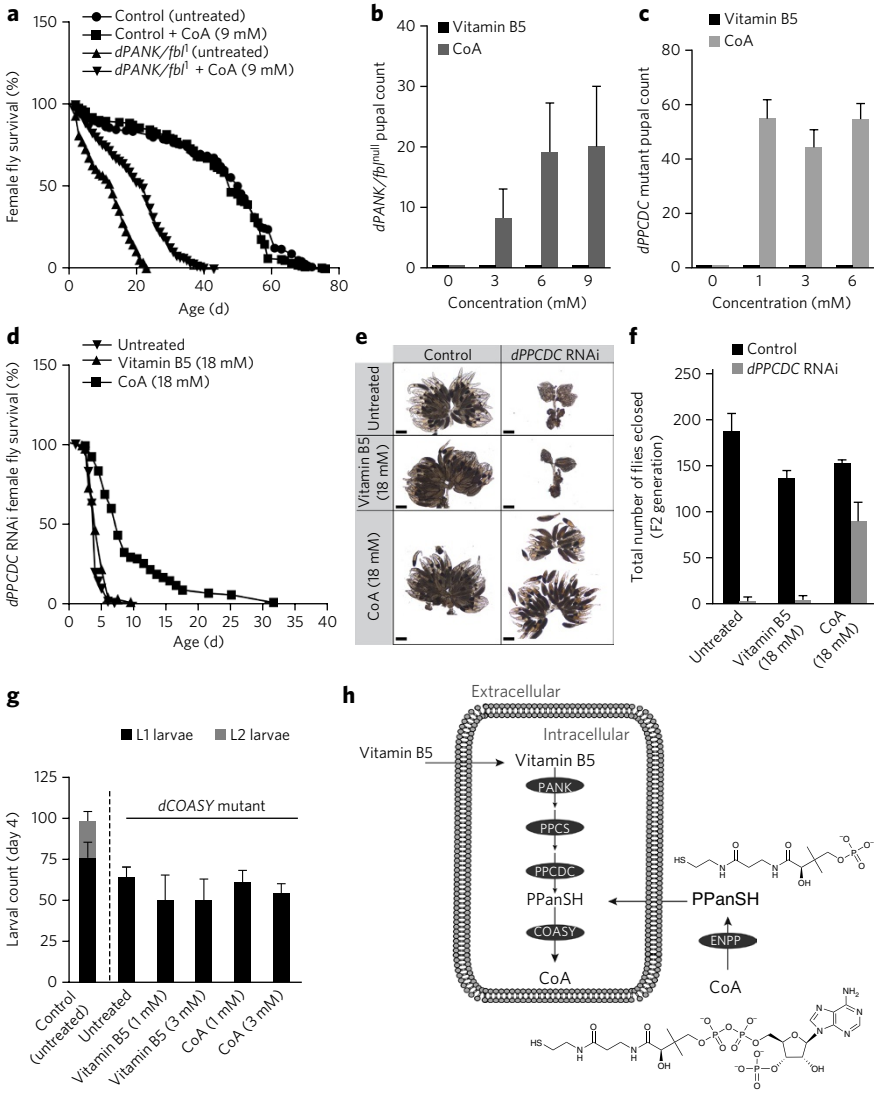

Figure 6 | External supplementation with CoA rescues *dPANK/fbl* and *dPPCDC* phenotypes but not *COASY*-impaired phenotypes. (**a**) Life-span analysis of *dPANK/fbl*^{1} mutants with (n = 260) and without (n = 207) CoA treatment compared with control flies with (n = 175) and without (n = 176) CoA treatment. Differences in survival curves between untreated and CoA-treated (9 mM) *dPANK/fbl*^{1} mutants were significant by log-rank (Mantel-Cox) test (P < 0.001). (**b**) Number of pupae of *dPANK/fbl*^{null} mutants after treatment with increasing concentrations of CoA or vitamin B5. (**c**) Number of pupae of *dPPCDC* mutants treated with CoA or vitamin B5. (**d**) Life-span analysis of the *dPPCDC* RNAi fly line untreated (n = 111) or treated with CoA (n = 102) or vitamin B5 (n = 102). Differences in survival curves between untreated and CoA-treated *dPPCDC* RNAi flies were significant by log-rank (Mantel-Cox) test (P < 0.001). (**e**) Ovaries of control and *dPPCDC* RNAi-expressing *Drosophila* females untreated or treated with CoA or vitamin B5, imaged with light microscopy. Scale bars, 200 µm. (**f**) Number of eclosed adult progeny of *dPPCDC* RNAi females crossed with control males raised on control food or supplemented with CoA or vitamin B5. (**g**) Number of L1 and L2 *dCOASY* mutant larvae and control larvae untreated or treated with CoA or vitamin B5. (**h**) Proposed noncanonical CoA supply route starting with extracellular CoA. PPanSH, 4′-phosphopantetheine. Data are mean and s.d. (n = 3) in **b**, **c**, **f** and **g**. Bars without error bars indicate that no pupae or eclosed flies were observed.

between cells and between membrane-bound cellular compartments. Our data further suggest that not all cells or organelles in an organism need to harbor all CoA biosynthetic enzymes to obtain CoA and that the route to CoA does not necessarily need to follow the archetypal path starting with the uptake of vitamin B5. Moreover, these observations hold promise for therapeutic intervention for PKAN, because 4′-phosphopantetheine is stable in serum and passes through cell membranes, thereby allowing for restoration of intracellular CoA levels in cells with defective CoA synthesis. The stability of 4′-phosphopantetheine is in strong contrast to characteristics of the dephosphorylated form, pantetheine, which is degraded rapidly in serum by pantetheinases into vitamin B5 and cysteamine[20,21]. These results show that the phosphate group protects the molecule from degradation and allows 4′-phosphopantetheine to serve as an effective substrate for CoA biosynthesis from its ready reserve in the circulation.

One intriguing question is whether the proposed route shown here has a physiological function or can be artificially provoked through manipulation of concentrations of extracellular CoA. Compared with CoA concentrations in cytoplasm (0.02–0.14 mM) and mitochondria (2.2–5.0 mM)[38], the concentrations used in our study (in the micromolar range) were relatively low. Answers may come from previous studies demonstrating that bacteria are able to excrete 4′-phosphopantetheine but not take it up from their environment, which suggests that bacteria-derived 4′-phosphopantetheine may be present in the digestive system of other organisms[39]. The presence of endogenous 4′-phosphopantetheine in mouse serum and in *dPANK/fbl*^{null} mutants is consistent with a possible source of extracellular 4′-phosphopantetheine. Such a 'ready' pool of CoA precursor may function in transport from one organ to another. In addition to being a source of intracellular CoA, extracellular CoA and 4′-phosphopantetheine may have signaling functions, as suggested by reports that CoA has effects on platelet aggregation and vasoconstriction[40,41]. Our results suggest that these effects, which have been attributed to CoA, may in fact be caused by 4′-phosphopantetheine. Future experiments are required to demonstrate the presence and possible effect of a net flow of CoA among organelles, cells and organisms (such as from intestinal bacteria to the host).

The ability of 4′-phosphopantetheine to translocate across membranes provides answers to long-standing questions regarding the intracellular distribution of CoA and its biosynthetic enzymes. CoA is present in the cytoplasm and in organelles such as mitochondria[38]. All CoA biosynthetic enzymes are present in cytoplasm[42], but only a subset have been found in mitochondria. It remains unclear how mitochondria obtain CoA, and the localization of COASY (but not the other CoA biosynthetic enzymes) to the mitochondrial matrix is also unexplained[17,43]. It has been postulated that CoA synthesized in the cytosol can be transported into the mitochondrial matrix by specific CoA transporters localized in the mitochondrial inner membrane[44]. Indeed, evidence for the presence of such CoA transporters has been presented[45]. On the basis of our observations, we hypothesize that 4′-phosphopantetheine is able to pass over the mitochondrial inner membrane and into the matrix and is subsequently converted into CoA by matrix COASY. This might explain the localization of COASY in the mitochondrial matrix[17,43].

The presence of a mechanism for 4′-phosphopantetheine uptake could have considerable implications for public health. Pathogens and parasites acquire resistance to treatments, and species-specific inhibitors of CoA biosynthetic enzymes are attractive candidates for a new class of antibiotics and antimalarial drugs[46,47]. Such inhibitors might be more effective antimicrobials when 4′-phosphopantetheine uptake is blocked as well. Alternatively, differences in the capacity for 4′-phosphopantetheine uptake by eukaryotic cells (as described in this article) and bacteria[39] may be further explored as possible targets for antimicrobial strategies.

CoA is essential for coordinating key aspects of cell function. It is therefore not surprising that an extracellular pool exists to facilitate swift replenishment and that it relies on the formation of a stable intermediate. Although these observations raise many new questions about CoA metabolism, they also suggest therapeutic approaches for a range of life-threatening human diseases.

Received 1 May 2015; accepted 3 August 2015;
published online 31 August 2015

METHODS

Methods and any associated references are available in the online version of the paper.

References

1. Baddiley, J., Thain, E.M., Novelli, G.D. & Lipmann, F. Structure of coenzyme A. *Nature* **171**, 76 (1953).
2. Strauss, E. Coenzyme A biosynthesis and enzymology. in *Comprehensive Natural Products II* (eds. Liu, H.-W. & Mander, L.) 351–410 (Elsevier, 2010).
3. Shi, L. & Tu, B.P. Acetyl-CoA induces transcription of the key G1 cyclin CLN3 to promote entry into the cell division cycle in *Saccharomyces cerevisiae*. *Proc. Natl. Acad. Sci. USA* **110**, 7318–7323 (2013).
4. Siudeja, K. *et al.* Impaired coenzyme A metabolism affects histone and tubulin acetylation in *Drosophila* and human cell models of pantothenate kinase associated neurodegeneration. *EMBO Mol. Med.* **3**, 755–766 (2011).
5. Takahashi, H., McCaffery, J.M., Irizarry, R.A. & Boeke, J.D. Nucleocytosolic acetyl-coenzyme A synthetase is required for histone acetylation and global transcription. *Mol. Cell* **23**, 207–217 (2006).
6. Choudhary, C. *et al.* Lysine acetylation targets protein complexes and co-regulates major cellular functions. *Science* **325**, 834–840 (2009).
7. Eisenberg, T. *et al.* Nucleocytosolic depletion of the energy metabolite acetyl-coenzyme A stimulates autophagy and prolongs lifespan. *Cell Metab.* **19**, 431–444 (2014).
8. Mariño, G. *et al.* Regulation of autophagy by cytosolic acetyl-coenzyme A. *Mol. Cell* **53**, 710–725 (2014).
9. McCoy, F. *et al.* Metabolic activation of CaMKII by coenzyme A. *Mol. Cell* **52**, 325–339 (2013).
10. Srinivasan, B. & Sibon, O.C. Coenzyme A, more than 'just' a metabolic cofactor. *Biochem. Soc. Trans.* **42**, 1075–1079 (2014).
11. Hoagland, M.B. & Novelli, G.D. Biosynthesis of coenzyme A from phospho-pantetheine and of pantetheine from pantothenate. *J. Biol. Chem.* **207**, 767–773 (1954).
12. Bosveld, F. *et al.* De novo CoA biosynthesis is required to maintain DNA integrity during development of the *Drosophila* nervous system. *Hum. Mol. Genet.* **17**, 2058–2069 (2008).
13. Daugherty, M. *et al.* Complete reconstitution of the human coenzyme A biosynthetic pathway via comparative genomics. *J. Biol. Chem.* **277**, 21431–21439 (2002).
14. Kupke, T., Hernandez-Acosta, P. & Culianez-Macia, F.A. 4′-phosphopantetheine and coenzyme A biosynthesis in plants. *J. Biol. Chem.* **278**, 38229–38237 (2003).
15. Zhyvoloup, A. *et al.* Molecular cloning of CoA synthase. The missing link in CoA biosynthesis. *J. Biol. Chem.* **277**, 22107–22110 (2002).
16. Shimizu, S., Kubo, K., Tani, Y. & Ogata, K. Purification and properties of pantothenate kinase from *Brevibacterium ammoniagenes* IFO 12071. *Biosci. Biotechnol. Biochem.* **37**, 2863–2870 (1973).
17. Dusi, S. *et al.* Exome sequence reveals mutations in CoA synthase as a cause of neurodegeneration with brain iron accumulation. *Am. J. Hum. Genet.* **94**, 11–22 (2014).
18. Zhou, B. *et al.* A novel pantothenate kinase gene (*PANK2*) is defective in Hallervorden-Spatz syndrome. *Nat. Genet.* **28**, 345–349 (2001).
19. Rana, A. *et al.* Pantethine rescues a *Drosophila* model for pantothenate kinase-associated neurodegeneration. *Proc. Natl. Acad. Sci. USA* **107**, 6988–6993 (2010).
20. Brunetti, D. *et al.* Pantethine treatment is effective in recovering the disease phenotype induced by ketogenic diet in a pantothenate kinase-associated neurodegeneration mouse model. *Brain* **137**, 57–68 (2014).
21. Wittwer, C.T., Gahl, W.A., Butler, J.D., Zatz, M. & Thoene, J.G. Metabolism of pantethine in cystinosis. *J. Clin. Invest.* **76**, 1665–1672 (1985).
22. Zhang, Y.M. *et al.* Chemical knockout of pantothenate kinase reveals the metabolic and genetic program responsible for hepatic coenzyme A homeostasis. *Chem. Biol.* **14**, 291–302 (2007).
23. Shibata, K., Nakai, T. & Fukuwatari, T. Simultaneous high-performance liquid chromatography determination of coenzyme A, dephospho-coenzyme A, and acetyl-coenzyme A in normal and pantothenic acid-deficient rats. *Anal. Biochem.* **430**, 151–155 (2012).
24. Novelli, G.D., Schmetz, F.J. Jr. & Kaplan, N.O. Enzymatic degradation and resynthesis of coenzyme A. *J. Biol. Chem.* **206**, 533–545 (1954).
25. Reilly, S.J., Tillander, V., Ofman, R., Alexson, S.E. & Hunt, M.C. The nudix hydrolase 7 is an Acyl-CoA diphosphatase involved in regulating peroxisomal coenzyme A homeostasis. *J. Biochem.* **144**, 655–663 (2008).
26. Shibata, K., Gross, C.J. & Henderson, L.M. Hydrolysis and absorption of pantothenate and its coenzymes in the rat small intestine. *J. Nutr.* **113**, 2107–2115 (1983).
27. Skrede, S. The degradation of CoA: subcellular localization and kinetic properties of CoA- and dephospho-CoA pyrophosphatase. *Eur. J. Biochem.* **38**, 401–407 (1973).
28. Trams, E.G., Stahl, W.L. & Robinson, J. Formation of S-acyl pantetheine from acyl-coenzyme A by plasma membranes. *Biochim. Biophys. Acta* **163**, 472–482 (1968).
29. Fernandez, N.J. & Kidney, B.A. Alkaline phosphatase: beyond the liver. *Vet. Clin. Pathol.* **36**, 223–233 (2007).
30. McLennan, A.G. The Nudix hydrolase superfamily. *Cell. Mol. Life Sci.* **63**, 123–143 (2006).
31. Rücker, B. *et al.* Biochemical characterization of ecto-nucleotide pyrophosphatase/phosphodiesterase (E-NPP, E.C. 3.1.4.1) from rat heart left ventricle. *Mol. Cell. Biochem.* **306**, 247–254 (2007).
32. Jansen, S. *et al.* Structure of NPP1, an ectonucleotide pyrophosphatase/phosphodiesterase involved in tissue calcification. *Structure* **20**, 1948–1959 (2012).
33. AbdelRaheim, S.R. & McLennan, A.G. The *Caenorhabditis elegans* Y87G2A.14 Nudix hydrolase is a peroxisomal coenzyme A diphosphatase. *BMC Biochem.* **3**, 5 (2002).
34. Grobben, B. *et al.* Ecto-nucleotide pyrophosphatase modulates the purinoceptor-mediated signal transduction and is inhibited by purinoceptor antagonists. *Br. J. Pharmacol.* **130**, 139–145 (2000).
35. Gu, X. *et al.* A new fluorometric turn-on assay for alkaline phosphatase and inhibitor screening based on aggregation and deaggregation of tetraphenylethylene molecules. *Analyst* **138**, 2427–2431 (2013).
36. Mensch, J. *et al.* Evaluation of various PAMPA models to identify the most discriminating method for the prediction of BBB permeability. *Eur. J. Pharm. Biopharm.* **74**, 495–502 (2010).
37. Rubio, S., Whitehead, L., Larson, T.R., Graham, I.A. & Rodriguez, P.L. The coenzyme A biosynthetic enzyme phosphopantetheine adenylyltransferase plays a crucial role in plant growth, salt/osmotic stress resistance, and seed lipid storage. *Plant Physiol.* **148**, 546–556 (2008).
38. Horie, S., Isobe, M. & Suga, T. Changes in CoA pools in hepatic peroxisomes of the rat under various conditions. *J. Biochem.* **99**, 1345–1352 (1986).
39. Jackowski, S. & Rock, C.O. Metabolism of 4′-phosphopantetheine in *Escherichia coli*. *J. Bacteriol.* **158**, 115–120 (1984).
40. Davaapil, H., Tsuchiya, Y. & Gout, I. Signalling functions of coenzyme A and its derivatives in mammalian cells. *Biochem. Soc. Trans.* **42**, 1056–1062 (2014).
41. Manolopoulos, P. *et al.* Acyl derivatives of coenzyme A inhibit platelet function via antagonism at P2Y1 and P2Y12 receptors: a new finding that may influence the design of anti-thrombotic agents. *Platelets* **19**, 134–145 (2008).
42. Skrede, S. & Halvorsen, O. Mitochondrial biosynthesis of coenzyme A. *Biochem. Biophys. Res. Commun.* **91**, 1536–1542 (1979).
43. Rhee, H.W. *et al.* Proteomic mapping of mitochondria in living cells via spatially restricted enzymatic tagging. *Science* **339**, 1328–1331 (2013).
44. Leonardi, R., Rock, C.O., Jackowski, S. & Zhang, Y.M. Activation of human mitochondrial pantothenate kinase 2 by palmitoylcarnitine. *Proc. Natl. Acad. Sci. USA* **104**, 1494–1499 (2007).
45. Fiermonte, G., Paradies, E., Todisco, S., Marobbio, C.M. & Palmieri, F. A novel member of solute carrier family 25 (SLC25A42) is a transporter of coenzyme A and adenosine 3′,5′-diphosphate in human mitochondria. *J. Biol. Chem.* **284**, 18152–18159 (2009).
46. Moolman, W.J., de Villiers, M. & Strauss, E. Recent advances in targeting coenzyme A biosynthesis and utilization for antimicrobial drug development. *Biochem. Soc. Trans.* **42**, 1080–1086 (2014).

47. Saliba, K.J. & Spry, C. Exploiting the coenzyme A biosynthesis pathway for the identification of new antimalarial agents: the case for pantothenamides. *Biochem. Soc. Trans.* **42**, 1087–1093 (2014).

Acknowledgments

This work was supported by the European Commission's Seventh Framework Programme (grant number FP7/2007-2013, HEALTH-F2-2011, grant agreement number 277984, TIRCON to V.T., H.P., S.H. and O.C.M.S.), a GUIDE research school grant (to B.S.), a VICI grant (NWO-grant 865.10.012 to O.S.) and Telethon GGP11088 (to V.T.). Part of the work was performed at the UMCG Microscopy and Imaging Center (UMIC), which is sponsored by NWO grant 175-010-2009-023. We thank P.G. Tepper and R. Van Merkerk (Pharmaceutical Biology, University of Groningen) for providing HPLC technical assistance and J.-W. Kok and D. Hoekstra (Department of Cell Biology, UMCG) for helpful discussions. We also thank T. de Boer and F. Oostebring from the Analytical Biochemical Laboratory BV (ABL, Assen, the Netherlands) for mass spectrometry analysis. We are grateful to the PKAN patients and their families who contributed samples to this study.

Author contributions

B.S., M.B., R.A.L., G.K., H.P., S.H., V.T. and O.C.M.S. designed the research. B.S., M.B., M.v.d.Z., B.K., C.C., R.A.L., O.S., A.P. and N.A.G. performed experiments. B.S., M.B., R.A.L. and O.C.M.S. analyzed results. E.A.A.N., G.K., H.P., S.H., V.T., D.-J.R., N.A.G. and O.C.M.S. supervised the research. B.S., N.A.G. and O.C.M.S. wrote the manuscript.

Competing financial interests

The authors declare competing financial interests: details accompany the online version of the paper.

Additional information

Supplementary information is available in the online version of the paper. Reprints and permissions information is available online at http://www.nature.com/reprints/index.html. Correspondence and requests for materials should be addressed to O.C.M.S.

ONLINE METHODS

***Drosophila* S2 cell culture, RNA interference, and CoA and 4′-phosphopantetheine treatment.** *Drosophila* Schneider's S2 cells were maintained at 25 °C in Schneider's *Drosophila* medium (Invitrogen) supplemented with 10% FCS (Gibco) and antibiotics (penicillin-streptomycin; Invitrogen) under laboratory conditions. Synthesis of RNAi constructs and double-stranded RNA (dsRNA) RNAi treatment were carried out as described previously[4]. Nonrelevant (human gene; *hMAZ*) dsRNA was used as a control. After incubating the cells for 4 d to induce efficient knockdown, we subcultured them with or without CoA (Sigma-Aldrich, C4780, 95%; used for all experiments) or 4′-phosphopantetheine (PPanSH) (Acies Bio, >92%) at different concentrations and maintained them for an additional 3 d until analysis for rescue efficiency of the compounds. The stock solutions of compounds were made in sterile water and stored at −20 °C until use.

HoPan treatment of *Drosophila* S2 cells in combination with CoA or PPanSH treatment. *Drosophila* Schneider's S2 cells were maintained under standard conditions as described above. Cells in the exponential phase of growth were used for all the experiments. Different concentrations of CoA or PPanSH (unlabeled or deuterium-labeled (PPanSH(D4)) were added to S2 cells in either the presence or the absence of 0.5 mM HoPan (Zhou Fang Pharm Chemical; 99%) for 48 h. Similarly, *Drosophila* S2 cells were treated with different concentrations of PPanSH(D4) at either 25 °C or 4 °C, and cells were then collected at various time points for analysis of of PPanSH(D4) transport. Stable isotope–labeled PPanSH containing four deuterium atoms was purchased as a sodium salt (Syncom; synthesized as previously described[48]; 99.7%). As readouts, we analyzed cell count, levels of intracellular total CoA and PPanSH (both labeled and unlabeled wherever appropriate) and histone acetylation as explained below.

***Drosophila* S2 cell immunofluorescence staining.** For immunofluorescence, *Drosophila* S2 cells were seeded on poly-L-lysine–coated (Sigma-Aldrich) glass microscope slides and allowed to settle for 45 min. Cells were fixed with 3.7% formaldehyde (Sigma-Aldrich) for 20 min, washed briefly with PBS + 0.1% Triton X-100 (Sigma-Aldrich) and permeabilized with PBS + 0.2% Triton X-100 for 20 min. We incubated the slides in primary antibody (rabbit anti-acLys, Cell Signaling, 9441, 1:500) in PBS + 0.1% Triton X-100 overnight to visualize histone acetylation levels, and after an additional washing step in PBS + 0.1% Triton X-100 we incubated the slides in secondary goat anti-rabbit conjugated to Alexa 488 (Molecular Probes) for 2 h at room temperature (RT). F-actin was detected with rhodamin-phalloidin (20 U/ml) (Invitrogen), and DNA was detected by staining with DAPI (0.2 µg/ml) (Thermo Scientific). Finally the samples were mounted in 80% glycerol and analyzed with a Leica fluorescence microscope with Leica software. Adobe Photoshop and Illustrator (Adobe Systems Incorporated, San Jose, California, USA) were used for image assembly.

HoPan treatment of mammalian HEK293 cells in combination with CoA and PPanSH treatment. HEK293 cells were maintained in DMEM (Invitrogen) supplemented with 10% FCS (Gibco) and antibiotics (penicillin-streptomycin, Invitrogen). For HoPan treatment, cells were cultured in custom-made DMEM without vitamin B5 (Thermo Scientific) supplemented with dialyzed FCS (Thermo Scientific). CoA or PPanSH was added to HEK293 cells to a final concentration of 25 µM, in either the presence or the absence of HoPan (0.5 mM), for 4 d, after which they were analyzed for phenotype and rescue efficiency of CoA and PPanSH.

Knockdown of COASY by siRNA in mammalian HEK293 cells. HEK293 cells were maintained as described above and transfected with 200 nM COASY short interfering RNA (siRNA) (GE Healthcare, human COASY 80347 smartpool, M-006751-00-0010) or non-targeting siRNA (GE Healthcare, D-001206-13-20) using Lipofectamine 2000 (Invitrogen). Four hours after transfection, CoA was added to a final concentration of 25 µM. Cells were cultured for 3 d and then collected for HPLC analysis of total CoA and PPanSH levels and western blotting (for histone acetylation) as described below.

Western blotting analysis and antibodies. For western blotting analysis, cells were collected, washed with PBS and centrifuged. The cells were lysed and sonicated in 1× Laemmli sample buffer and boiled for 5 min with 5% β-mercaptoethanol (Sigma). Protein content was determined via DC protein assay (Bio-Rad). Equal amounts of protein were loaded on a 10% or 12.5% SDS-PAGE gel, transferred onto PVDF membranes and blocked with 5% milk in PBS + 0.1% Tween, after which they were incubated overnight with primary antibodies. The primary antibodies used were rabbit anti-dPANK/fbl (1:4,000, Eurogentec, custom made as described previously[12]), mouse anti-tubulin (Sigma-Aldrich, T5168, 1:5,000), anti–acetyl-Histone3 (Active Motif, 39139, 1:2,000), anti-GAPDH (Fitzgerald, 10R-G109a, 1:10,000), and rabbit anti-COASY (Abcam, AB129012, 1:1,000). Appropriate horseradish peroxidase–conjugated secondary antibodies (Amersham) were used, and detection was performed using enhanced chemiluminescence (Pierce, 32106) and Amersham hyperfilm (GE Healthcare). Band intensities were quantified with Image Studio software. Full uncut gel images for all western blots are shown in **Supplementary Figures 15** and **16**.

***C. elegans* media and strains.** Standard culturing conditions were used for *C. elegans* maintenance at 20 °C. The N2 strain was used as a wild-type control. VC927, the PANK-deletion mutant *pnk-1 (ok1435)I/hT2[bli-4(e937) let-? (q782) qIs48](I;III)*, was obtained from the *Caenorhabditis* Genetics Center. To obtain synchronous cultures, we bleached worms with hypochlorite, allowed them to hatch in M9 buffer (3 g KH_2PO_4, 6 g Na_2HPO_4, 5 g NaCl, 1 ml 1 M $MgSO_4$, H_2O to 1 l) overnight, and cultured them on standard nematode growth medium (NGM) plates seeded with the OP50 strain of *Escherichia coli*.

***C. elegans* life-span assay.** After synchronization, *C. elegans* L1 animals were grown on control NGM plates or NGM plates supplemented with 400 µM CoA. We started the life-span experiments by transferring 100 one-day-old adults per condition onto NGM plates that contained 5-fluoro-2′-deoxyuridine to inhibit the growth of offspring. Surviving animals were counted once a day; worms that disappeared or crawled out of the plate were excluded from the analysis.

***C. elegans* motility assay.** After synchronization, L1 *C. elegans* were grown on control NGM plates or NGM plates containing various concentrations of CoA. One-day-old adults were placed in a drop of M9 buffer and allowed to recover for 30 s. During the subsequent 30 s, we counted the number of body bends. A movement was scored as a bend when both the anterior and posterior ends of the animal turned to the same side. At least 15 worms were scored per condition, and each experiment was repeated thrice. Sequential light microscopy images demonstrating movements of *C. elegans* in M9 buffer were captured using a Leica MZ16 FA microscope at 32× magnification within a time frame of 1 s and were processed using ImageJ (US National Institutes of Health) and Adobe Photoshop.

***Drosophila* maintenance and crosses.** *D. melanogaster* stocks and crosses were raised on standard cornmeal agar fly food (containing water, agar (17 g/L), sugar (54 g/L), yeast extract (26 g/L) and nipagin (1.3 g/L)) at 25 °C. The stocks were obtained from the Bloomington Stock Center (Indiana University, USA), the VDRC (Vienna *Drosophila* RNAi Collection, Vienna, Austria) or the Exelixis Collection (Harvard Medical School) and rebalanced over eGFP-positive balancers for identification of homozygous (eGFP-negative) progeny. The stocks used were *w[1118]*; *dPANK/fbl*^{1} hypomorph[12,19]; *dPANK/fbl*^{null} (y[1] w[*]; *Mi{y[+mDint2] = MIC}fbl[MI04001]/TM3, Sb[1] Ser[1]*, Bloomington 36941); *dPPCDC* mutant (*w[1118]; PBac{w[+mC] = WH}Ppcdc[f00839]/CyO*, Bloomington 18377); UAS-*dPPCDC* RNAi line (VDRC 104495); and *dCOASY* mutant (*PBac{RB}Ppat-Dpck[e00492]*, Exelixis). The UAS-RNAi constructs were expressed ubiquitously with the *Actin-Gal4* drivers (*y[1] w[*]; P{w[+mC] = Act5C-GAL4}25FO1/CyO, y[+]*, Bloomington 4414). As controls we used heterozygous flies or larvae for the mutants and the Actin-Gal4 driver crossed to isogenic w^{1118} flies (*Actin-Gal4/+*) for the RNAi construct–expressing flies.

***Drosophila* larval collection and counts.** One-week-old flies (ten females and five males) were kept on 5 ml of standard fly food in a vial at 25 °C with or without various concentrations of CoA or vitamin B5 (Sigma, P5155). The flies were allowed to lay eggs for 2 d, and the parent flies were then discarded. The L1, L2 and L3 larvae were collected from the food with 20% sucrose at the appropriate time (days 4, 6 and 8, respectively) for larval counting and stored at −80 °C until analysis. The pupal count was taken between days 10 and 12.

***Drosophila* HoPan toxicity and CoA rescue.** One-week-old w^{1118} flies (ten females and five males) were kept in vials containing standard fly food with or without HoPan and CoA. The flies were allowed to lay eggs for 2 d, after which

the adults were discarded. The resulting offspring were allowed to develop. We counted the numbers of flies that eclosed to evaluate HoPan toxicity and CoA rescue efficiency.

***Drosophila* life span.** One-day-old female adult flies of *Drosophila* homozygous mutant or RNAi construct–expressing lines were collected with appropriate controls and kept on standard fly food at 25 °C with or without CoA or vitamin B5 (Sigma) at various concentrations (in 50 µl added on top of the fly food and allowed to dry before flies were introduced). The flies were counted every 12–24 h and flipped to new fly food vials containing the same amount of CoA or vitamin B5.

***Drosophila* ovary rescue experiment.** UAS–*dPPCDC* RNAi constructs were ubiquitously expressed under the control of *Actin-Gal4*. The crosses were raised at 25 °C. F1 RNAi construct–expressing females and control females were collected shortly after eclosion and transferred to standard fly food or food containing vitamin B5 or CoA (18 mM). Flies were maintained for 2 d on this food at 25 °C. After this period, extra yeast and w^{1118} control males were added, and the crosses were kept at 25 °C for another 2 d. After this 4-d period, we dissected out ovaries from the female flies and stained them for further analysis. The vials (or plates) from the crosses (with eggs that were being laid during the 4-d period of CoA treatment) were kept for another 10 d, and offspring were counted after eclosion.

RNA isolation, quantitative real-time PCR, and primers. *Drosophila* larvae and samples of 1-d-old adult flies or larvae were collected for homozygous *dPPCDC* mutants, *dPPCDC* RNAi construct–expressing lines and homozygous *dCOASY* mutants and washed briefly with PBS. The samples were lysed in TRIzol (Invitrogen) for RNA extraction and reverse-transcribed using M-MLV (Invitrogen) and oligo(dt) 12-18 (Invitrogen). SYBR green (Bio-Rad) and Bio-Rad real-time PCR with specific primers were used for analyses of gene expression level. The expression levels were normalized for *rp49* (housekeeping gene). The primer sequences used were as follows: *dPPCDC*, TGCACCTGCGATGAATACCC, TCGGCTGAAAGGCGG ATAAC; *dCOASY*, GGCTGTGCGGCGGATTATTG, CGGGTTAAAGGCTGC TCTGG; and *rp49*, GCACCAAGCACTTCATCC, CGATCTCGCCGCAGT AAA (Biolegio).

***Drosophila* ovary dissection and staining.** *Drosophila* ovaries were collected in cold PBS and fixed in 4% formaldehyde (from methanol-free 16% formaldehyde solution, Thermo Scientific) for 45 min at RT. The fixed tissue was washed in PBS + 0.1% Triton X-100 for 1 h at RT and then permeabilized in PBS + 0.2% Triton X-100 for 1 h. We stained the ovaries with rhodamin-phalloidin (20 U/ml) to detect F-actin and with DAPI (0.2 µg/ml) to detect DNA. Finally the samples were mounted in 80% glycerol and analyzed on a Zeiss-LSM780 NLO confocal microscope with Zeiss Zen software. Adobe Photoshop and Adobe Illustrator were used for image assembly.

PAMPA procedure. PAMPA was performed and processed according to the manufacturer's instructions (BD Gentest pre-coated PAMPA plates). Briefly, two superimposed wells were separated by an artificial lipid-oil-lipid membrane. The compound of interest (PPanSH, CoA, caffeine or amiloride) was added to the bottom well in PBS, and the top well was filled with PBS alone. After 5 h of incubation at RT, we measured concentrations of the different compounds using UV-VIS absorption spectroscopy (BMG Labtech SPECTROstar Omega) and calibration curves for all compounds. We calculated the permeability efficiency according to the manufacturer's instructions (**Supplementary Fig. 9e**). For caffeine and amiloride, 4 replicates were performed; for PPanSH and CoA, 12 replicates were performed. Caffeine and amiloride were obtained from Sigma.

Serum collection from PKAN patients. We collected serum from the blood of PKAN patients and respective healthy family members (controls) using standard protocols. Briefly, venous blood was collected in commercially available red-topped Vacutainer tubes (Becton Dickinson) and allowed to remain at RT undisturbed for 15–30 min for blood clotting. The tubes were then centrifuged at 2,000*g* for 10 min at 4 °C. The resulting supernatant serum was immediately transferred to 2-ml cryovials and maintained at −80 °C until CoA stability assessments were performed. Blood samples and clinical data were obtained according to Oregon Health and Science University's institutional review board–approved repository protocol 7232 with the informed consent of participating subjects.

CoA and pantethine serum-stability measurements. CoA serum-stability studies were conducted in commercially obtained serum and in serum collected from PKAN patients and related healthy controls. Human and mouse sera were purchased from Sigma, and FCS was purchased from Gibco. Additionally, DMEM with or without 10% FCS was used for evaluation of CoA stability. Briefly, all sera and samples were incubated for 30 min at 37 °C with or without preconditioning compounds at a final concentration of 10 mM (adenosine 5′-triphosphate (ATP), adenosine 5′-diphosphate (ADP), EDTA, levamisole, suramin, DIDS and NaF, all purchased from Sigma), and then CoA (20 µM) was added at a ratio of 1:1 and the mixture was incubated at 37 °C after brief vortexing. For heat inactivation, all sera were incubated for 30 min at 56 °C, after which CoA was added. At different time points, serum samples were collected, deproteinized and analyzed by HPLC as described below. For pantethine serum stability, pantethine (Sigma) was incubated in FCS, mouse serum and human serum for 15 min at 37 °C, and total levels of pantetheine and cysteamine were measured via HPLC.

Intravenous injection of CoA in mice. Adult male mice of C57BL/6J 129/SvJ mixed genetic background were used for this study. Two mice (approximately 25–30 g in weight) were used for each condition. We injected 0.1 mg or 0.5 mg CoA in 0.25 ml saline solution intravenously into the tail vein. Saline solution (0.25 ml) was injected in control groups. After 30 min and 6 h, blood samples were collected and further processed to obtain plasma, and then samples were prepared for HPLC or LC-MS analysis as indicated below. All animal studies were approved by the Ethics Committee of the Foundation IRCCS Neurological Institute C. Besta, in accordance with guidelines of the Italian Ministry of Health, Project No. BT4/2014. The use and care of animals followed Italian Law D.L. 116/1992 and EU directive 2010/63/EU.

HPLC sample-preparation protocol for measurement of total CoA and PPanSH. Samples were briefly washed with ice-cold PBS solution. We sonicated samples thoroughly in 100 µl of ice-cold PBS and centrifuged them for 10–15 min at 4 °C to collect supernatant. Tris(2-carboxyethyl)phosphine hydrochloride (Sigma) (50 mM; 10 µl) was added to 50 µl sample supernatant and incubated at RT for 15 min after vortex-mixing. Saturated ammonium sulfate solution or Millipore 3KD centrifugal filter units were used to remove proteins. The samples were centrifuged at 14,000 rpm for 15 min at 4 °C. The clear supernatant (50 µl) or the filtrate was derivatized with 45 µl of ammonium 7-flurobenzo-2-oxa-1,3-doazole-4-sulfonate (SBD-F, Sigma) (1 mg/ml in borax buffer, 0.1 M containing 1 mM EDTA disodium, pH 9.5) and 5 µl of ammonia solution (12.5% vol/vol, Merck Millipore) at 60 °C for 1 h. The derivatized samples were placed in a refrigerated autosampler (10 °C) in the Shimadzu HPLC system and injected for total CoA and PPanSH analysis using optimized chromatographic separation conditions combined with fluorescence detection (described below).

Chromatography separation condition. Chromatographic analysis was performed with a Shimadzu LC-10AC liquid chromatograph, SCL-10A system controller, SIL-10AC automatic sample injector and LC-10AT solvent-delivery system. A Shimadzu RF-20Axs fluorescence detector was used for derivatized sample extract analysis. The fluorescence detector was set at excitation and emission wavelengths of 385 nm and 515 nm, respectively. Signal output was collected digitally with Shimadzu Labsolution software, and post-run analyses were performed. Chromatographic separation of the analytes was achieved with a Phenomenex Gemini C18 guard column (4 × 3 mm) connected to a Phenomenex Gemini NX-C18 analytical column (4.6 × 150 mm; 3-µm particles) at 45 °C. The two mobile phases consisted of (A) 100 mM ammonium acetate buffer (pH 4.5) and (B) acetonitrile. The flow rate was maintained at 0.8 ml/min with a slow gradient elution: 0% B until 7 min, 20% B at 20 min, 20% B at 22 min, 50% B at 23 min, maintained at 50% B until 27 min, 0% B at 28 min, and 7–10 min for column re-equilibration.

Sample preparation for mass spectrometry and instrument parameters. Samples were briefly washed with ice-cold PBS solution. Samples were then sonicated thoroughly in 100 µl of ice-cold milliQ (MQ) water containing

doi:10.1038/nchembio.1906

50 mM Tris(2-carboxyethyl)phosphine hydrochloride. Subsequently we added 100 µl of saturated ammonium sulfate to each sample and centrifuged the samples for 20 min at 10 °C and 16,100*g* to collect supernatant. We added 15 µl of ammonium hydroxide (12.5%) to 150 µl of supernatant and injected 20 µl of the mixture for LC-MS analysis. For mouse plasma analysis, we added 50 µl of MQ water containing 50 mM Tris(2-carboxyethyl)phosphine hydrochloride to 50 µl of plasma and processed it further as described above. Appropriate dilution series of standard CoA, PPanSH and PPanSH(D4) were processed similarly before analysis. The LC separations of metabolites were obtained with a Phenomenex Gemini NX-C18 analytical column (4.6 × 150 mm; 3-µm particles) at 45 °C. The flow was maintained at 1 ml/min with an optimized mobile phase gradient of MQ water (A), 200 mM ammonium acetate (NH_4Ac) in 95%/5% MQ water/acetonitrile adjusted to pH 4.5 with acetic acid (B), and acetonitrile (C). The separated analytes were detected with positive-mode mass spectrometry (Sciex API5500 Q-trap) under unit resolution. The targeted Q1/Q3 mass/charge values of PPanSH, PPanSH(D4), CoA and CoA(D4) were 359.1/261.1, 363.1/265.1, 768/261.1 and 772/265.1, respectively. The absolute concentration was calculated via linear regression analysis of the respective standard compounds, except that of CoA(D4), which was estimated indirectly using CoA standards.

Statistical analysis. All experimental results are presented as the mean of at least three independent experiments ± s.d., unless otherwise stated. Statistical significance was determined by two-tailed unpaired Student's *t*-test between appropriate groups wherever applicable. For life-span survival curves, more than 80 flies or *C. elegans* were used in each group, and statistical significance was determined via log-rank (Mantel-Cox) test (exact numbers of flies and *C. elegans* used for survival analysis are stated in figure legends). Statistical *P* values of ≤0.05 were considered significant. Data were analyzed using GraphPad Prism (GraphPad Software, San Diego, CA, USA).

48. Mandel, A.L., La Clair, J.J. & Burkart, M.D. Modular synthesis of pantetheine and phosphopantetheine. *Org. Lett.* **6**, 4801–4803 (2004).